Journal of Alloys and Compounds 509 (2011) 1261–1265

Contents lists available at ScienceDirect

Journal of Alloys and Compounds

journal homepage: www.elsevier.com/locate/jallcom

Microwave-assisted synthesis and magnetic properties of size-controlled CoNi/MWCNT nanocomposites

Huaqiang Wu*, Peipei Cao, Wenting Li, Na Ni, Lulu Zhu, Xiaojun Zhang

College of Chemistry and Materials Science, Anhui Key Laboratory of Functional Molecular Solids, Anhui Normal University, Wuhu 241000, PR China

ARTICLE INFO

Article history:
Received 13 August 2010
Received in revised form
27 September 2010
Accepted 30 September 2010
Available online 14 October 2010

Keywords:
CoNi alloy
Carbon nanotubes
Magnetic properties
Microwave

ABSTRACT

Size-controlled CoNi alloy nanoparticles with average diameters in the range of 15–48 nm attached on the multi-walled carbon nanotubes (MWCNTs) were prepared to form CoNi/MWCNT nanocomposites by microwave-assisted method. The size of CoNi alloy nanoparticles can be controlled through adjusting the atomic ratios of metals to carbon nanotubes in the mixed acetate solution. The as-prepared nanocomposites have been characterized by X-ray powder diffraction (XRD), scanning electron microscopy (SEM), transmission electron microscopy (TEM), high-resolution transmission electron microscopy (HRTEM), selected area electron diffraction (SAED), energy-disperse X-ray spectroscopy (EDS) and vibrating sample magnetometer (VSM). The results show that CoNi alloy nanoparticles are face-centered cubic structure, quasi-spherical and disperse uniformly on the surface of MWCNTs. Magnetic measurement shows that both the coercivity and the saturation magnetization of the samples increase with the increase of the particle size from 15 to 37 nm, and decrease from 37 to 48 nm.

1. Introduction

Magnetic nanoparticles have important applications as catalysts, magnetic fluids, and high-density recording media. As important transition metal alloys, CoNi alloys have been widely used for decoration, corrosion resistance and magnetic recording devices, and catalysts, etc. [1–5]. In such applications, composition of CoNi alloy nanoparticles is considered the key characteristic affecting their magnetic properties and has been investigated by different methods [6–9]. In addition to the composition, the shape and size of the magnetic nanoparticles are also key factors in the applications mentioned above. Recently, shape- and size-controlled synthesis of the magnetic nanoparticles has been an active research area owning to their shape- and size-dependent electrical, optical and magnetic properties [10–12]. For example, magnetic recording density is remarkably enhanced as the size of magnetic particles decreases. CoNi alloy nanoparticles with different shapes and sizes have been prepared such as nanowires [13,14], bracelet-like [15], chain-like [16], handkerchief-like [6], and film [3,17], etc.

The multi-walled carbon nanotubes (MWCNTs) have been widely applied as a promising support material in many areas of science and technology due to their specific characteristics such as large surface area to volume ratio, good adsorption, unique structure, and high thermal and chemical stability. As is well-known, there have been various approaches to deposit monometal magnetic nanoparticles such as Ni [18], Co [19], Fe [20], Fe_2O_3 [21] and Fe_3O_4 [22] on the surface of MWCNTs by microwave irradiation heating method, chemical precipitation and deoxidization method, pyrolysis of ferrocene, chemical precipitation, and by using ethylene glycol as reductant, respectively. In these methods, microwave-assisted synthesis has remarkable advantages of short reaction time, small particle size, narrow particle size distribution, high purity of the products and eco-friendly. In our previous work [23,24], we found that microwave-assisted synthesis in the deposition of nanoparticles onto MWCNTs is a very useful and powerful method to directly control the size, morphology, structure, and loading of nanoparticles.

In this work, we attempted to extend this microwave-assisted method to prepare size-controlled CoNi alloy nanoparticles attached on the outer surface of the MWCNTs and to study the effect of the change in the size of CoNi alloy nanoparticle on the magnetic properties. Experimental results demonstrated that CoNi alloy nanoparticles with quasi-spherical and face-centered cubic structure have been attached on the MWCNTs. The size of CoNi alloy nanoparticles with an average diameter of 15–48 nm can be controlled through adjusting the atomic ratios of metals to carbon nanotubes (3, 7, 12, and 18 at%, respectively) in the mixed acetate solution. Magnetic measurement confirmed that both the coercivity (*Hc*) and the saturation magnetization (*Ms*) of the samples first increase with the increase of the size, then decrease with the increase of the size of CoNi alloy nanoparticles on the MWCNTs. Moreover, a possible mechanism of formation was discussed.

* Corresponding author.
E-mail address: wuhuaq@mail.ahnu.edu.cn (H. Wu).

0925-8388/$ – see front matter © 2010 Elsevier B.V. All rights reserved.
doi:10.1016/j.jallcom.2010.09.209

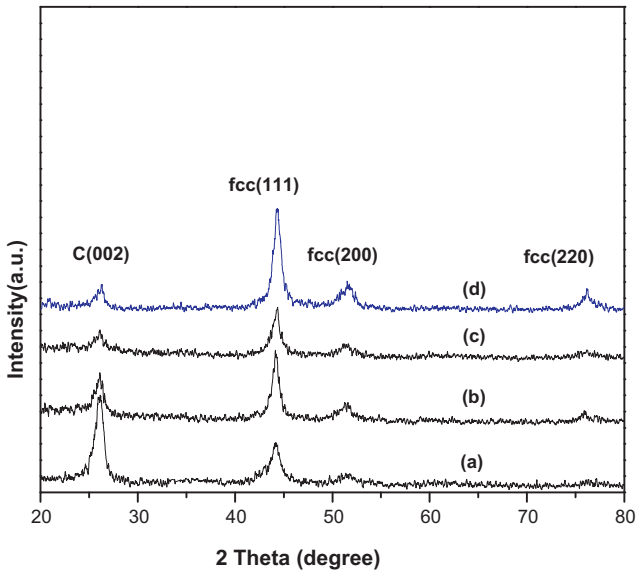

Fig. 1. The XRD patterns of different atomic ratios (a) 3 at%, (b) 7 at%, (c) 12 at%, (d) 18 at% of metals to carbon nanotubes

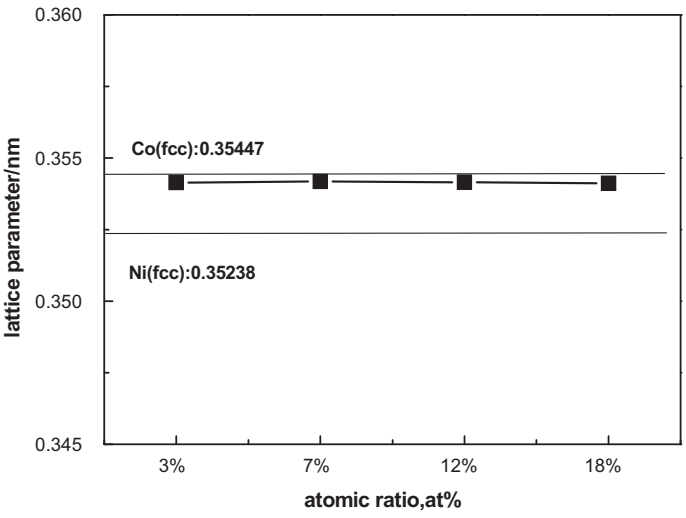

Fig. 2. Lattice parameters of different atomic ratios calculated from the XRD pattern

2. Experimental

The MWCNTs with a purity of about 95% were provided by Shenzhen Nanoport Company, which were produced via catalytic decomposition of hydrocarbon. For the better anchoring of the nanoparticles, the MWCNTs were refluxed in concentrated nitric acid for 4 h, then purified by distilled water, and finally dried at 100 °C for 24 h. All chemicals were of analytical grade and used as received without further purification. In a typical synthesis, 0.0300 g of the acid-treated MWCNTs was mixed with 0.0187 g of $Co(Ac)_2 \cdot 4H_2O$ and 0.0187 g of $Ni(Ac)_2 \cdot 4H_2O$ (Co:Ni = 1:1 atomic ratio) in ethylene glycol (25 mL). After stirring the mixture for 24 h, an appropriate NaOH solution was added to the mixture to adjust the pH to 10. Simultaneously, several drops of hydrazine hydrate were added as a reducing agent. Subsequently, the mixture was added in a 100 mL round-bottom bottle, which was placed in a microwave refluxing system (National N-S570MFS microwave oven, 2450 MHz, 900 W, Sanle General Electric Corp. Nanjing, China) at 600 W for 2 min. The as-obtained samples were washed with distilled water and absolute ethanol several times to remove possible residual impurities. The products were dried at 60 °C in a vacuum oven before being further characterized. By varying the atomic ratios of the metals to carbon nanotubes, different atomic ratios (3, 7, 12 and 18 at%) of CoNi/MWCNT nanocomposites were prepared according to the above methods.

The as-obtained samples were characterized by X-ray powder diffraction (XRD) on an XRD-6000 (Japan) X-ray diffractometer with Cu-Kα radiation (λ = 0.154060 nm) at a scanning rate of 0.05° s^{-1} in the 2θ range from 20° to 80°. The morphology and size of as-obtained products were observed by transmission electron microscopy (TEM) carried out on a Hitachi H-800 transmission electron microscope and scanning electron microscopy (SEM) operated on a Hitachi S-4800 scanning electron microscope. High-resolution transmission electron microscopy (HRTEM) and selected area electron diffraction (SAED) were performed using JEM 2010F field emission microscope operated at optimum defocus with accelerating voltages of 200 kV. Energy-dispersive X-ray spectrometry (EDS) was carried out with spectroscope attached to HRTEM, which was used for elemental analysis. The magnetic hysteresis loop of sample was measured by vibrating sample magnetometer (VSM, BHV-55, Japan) with an applied field ± 10 kOe at room temperature.

3. Results and discussion

3.1. Characterization of the samples

Fig. 1 shows the XRD patterns of different atomic ratios of metals to carbon nanotubes (3, 7, 12 and 18 at%) samples at room temperature. The peak at 2θ value of 26.13° arising from the carbon nanotubes corresponds to its (0 0 2) crystal plane. The peaks at 2θ values of 44.38°, 51.48°, and 76.45° correspond to the crystal planes of the (1 1 1), (2 0 0), and (2 2 0) of face-centered cubic (fcc) CoNi nanoparticle, which are in good accordance with reported literature value [6]. The cell parameters were calculated from the XRD pattern and the results were displayed in Fig. 2. It can be seen that the cell parameter of CoNi nanoparticle is nearly a consent (0.35416 nm) and larger than that of fcc Ni (0.35238 nm) and smaller than that of fcc Co (0.35447 nm) [25], this confirms that CoNi nanoparticle is fcc phase. And there were no observable peaks in the XRD spectra corresponding to those of pure cobalt and nickel, so the homogeneous solid solution of CoNi should have been formed. These facts confirm that Co and Ni formed an alloy, rather than separate grains [16]. The average crystallite size for different atomic ratios (3, 7, 12, and 18 at%) of CoNi/MWCNTs, calculated using the Debye–Scherrer formula based on the full width at half-maximum of the (1 1 1) diffraction peak, was 12.1, 21.2, 36.9, and 42.5 nm, respectively.

Fig. 3 shows the morphology and microstructure of the different atomic ratios of CoNi/MWCNTs examined by SEM and TEM. It can be seen that the quasi-spherical CoNi alloy nanoparticles are attached uniformly on the surface of carbon nanotubes. As a whole, the loading of the CoNi alloy nanoparticles attached on the carbon nanotubes increases with increasing the atomic ratios of metals to carbon nanotubes. The average size of the alloy nanoparticles from the TEM images were 15, 25, 37, and 48 nm, which corresponds to 3, 7, 12, and 18 at%, respectively, which is consistent with the trend of the change in the crystallite size calculated from the Debye–Scherrer formula. The size of CoNi alloy nanoparticles increases with increasing the atomic ratios of metals to carbon nanotubes (listed in Table 1), and the loading of CoNi alloy nanoparticles increased, even with a denser layer of CoNi nanospheres when the atomic ratio was 18 at% as shown in Fig. 3(g) and (h).

HRTEM is employed to investigate the inner structure of CoNi/MWCNT nanocomposites (Fig. 4(a)), showing well-defined lattice fringes of CoNi nanoparticles. The measured spacing of the crystallographic planes is 0.204 nm and 0.342 nm from the HRTEM images, corresponding to the (1 1 1) and (0 0 2) plane separations of CoNi and MWCNTs, respectively. The SAED (Fig. 4(b)) can reveal details of the local CoNi structure, which can be indexed

Table 1
Magnetization data for different atomic ratios of CoNi/MWCNT nanocomposites measured at room temperature.

Metal (CoNi) to carbon nanotubes atomic ratios (at%)	Crystallite size (nm)	*Hc* (Oe)	*Ms* (emu/g)
3	15	260.5	14.1
7	25	405.6	33.0
12	37	421.8	46.1
18	48	384.1	25.8

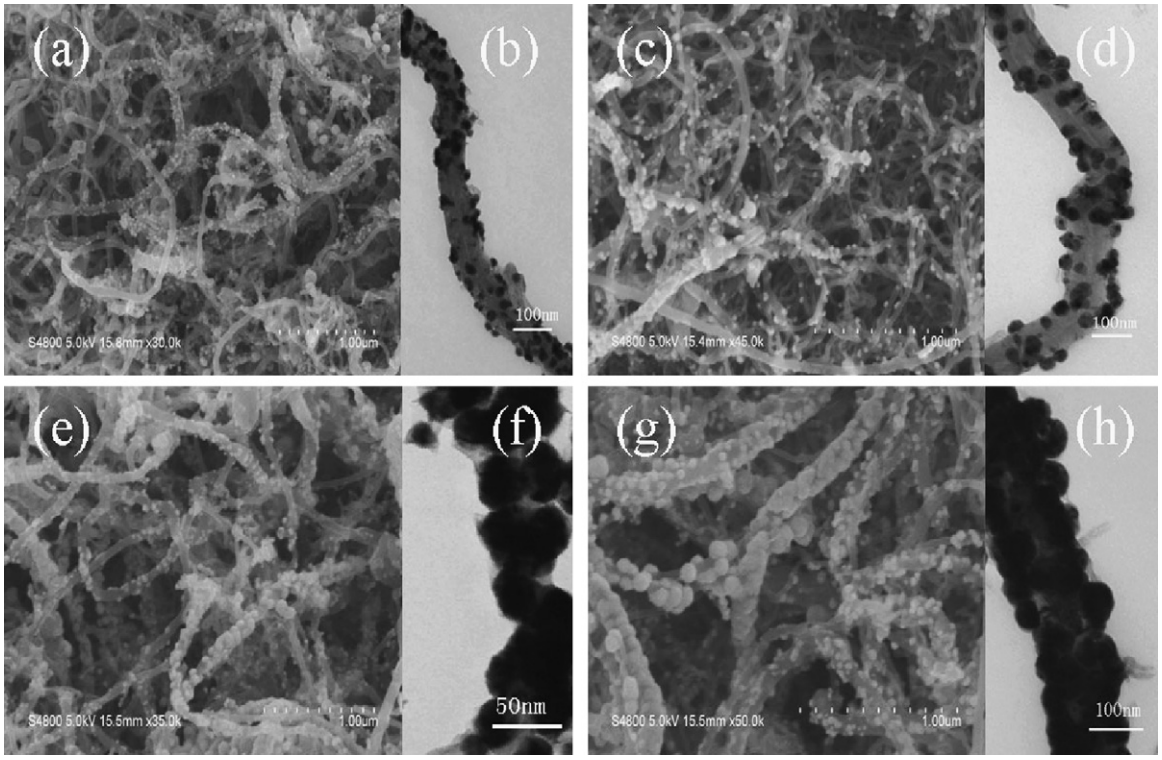

Fig. 3. SEM and TEM images of the as-prepared nanocomposites (a and b) 3 at%, (c and d) 7 at%, (e and f) 12 at%, and (g and h) 18 at%

to polycrystalline CoNi. The concentric rings could be assigned as diffractions from the (1 1 1), (2 0 0), and (2 2 0) planes of fcc CoNi, and the centermost ring is assigned as diffractions from the (0 0 2) plane of MWCNTs, which is consistent with the XRD results. The EDS spectrum (Fig. 4(c)) shows the presence of Co, Ni, Si and C, which confirms the existence of CoNi on MWCNTs. It is obvious that the silicon peak is caused by the silicon chip used to clamp the nanoparticles. The carbon comes from the carbon nanotubes. The oxygen peak in the spectrum probably originates from the unavoidable surface-adsorption of oxygen onto the samples from exposure to air during sample processing. The atomic ratio of Co to Ni for the majority of CoNi alloy nanoparticle is 0.47:0.53 according to EDS quantitative microanalysis, which is close to the stoichiometry of CoNi.

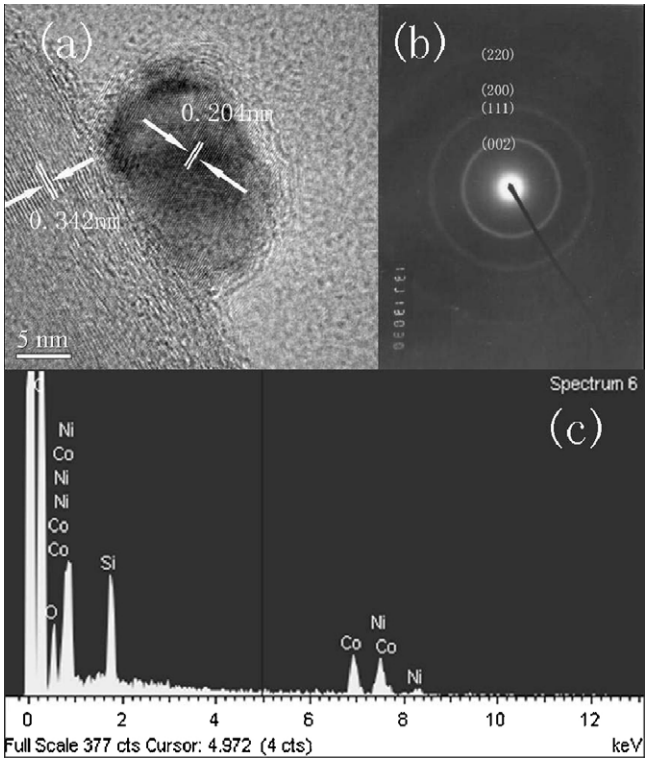

Fig. 4. (a) HRTEM image, (b) SAED pattern and (c) EDS spectrum of the obtained CoNi/MWCNT nanocomposites

3.2. Possible formation mechanism

In our experiments, the morphology and size of the samples were found to be strongly depended on the experimental conditions such as the microwave power, the reaction time and the atomic ratios of CoNi/MWCNTs. By adjusting these experimental parameters suitably, the size of CoNi alloy nanoparticles will be controlled. It has been found that when the reaction time is less than 2 min, the MWCNTs are coated with fewer CoNi nanoparticles unevenly. When the reaction time is longer than 2 min, the severely aggregated CoNi nanoparticles on the MWCNTs are obtained. The size of CoNi alloy nanoparticles increased with increasing the microwave power. Therefore, we chose the proper condition that the microwave power was 600 W and the reaction time was 2 min, CoNi alloy nanoparticles were dispersed uniformly on the surface of MWCNTs under this condition. Except for the factors above, the atomic ratio of CoNi/MWCNTs was a crucial factor for the size of CoNi alloy nanoparticles, we found that the size of CoNi alloy nanoparticles increased with increasing the atomic ratios of CoNi/MWCNTs.

Based on our experimental results, a possible formation and growing mechanism of CoNi/MWCNT nanocomposites can be proposed as follows: the positive metal ions Co^{2+} and Ni^{2+} can be adsorbed effectively onto the surface of the acid-treated MWCNTs via electrostatic attraction, then positive metal ions Co^{2+} and Ni^{2+}

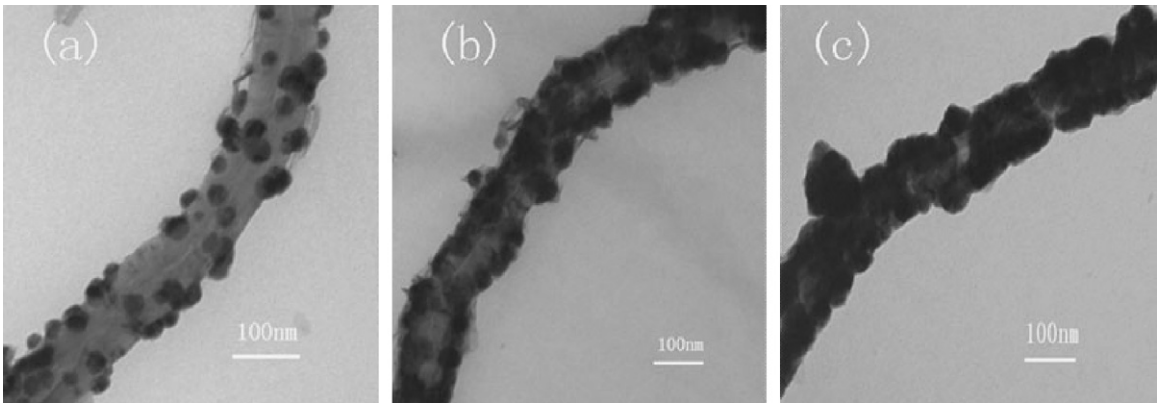

Fig. 5. TEM images of CoNi/MWCNT nanocomposites obtained with the different atomic ratios (a) 7 at%, (b) 12 at%, (c) 18 at%

were reduced by hydrazine hydrate due to the microwave irradiation, metallic cobalt and nickel formed CoNi alloy nanoparticles. The reactions can be expressed as Eqs. (1), (2), and (3).

$$2Ni^{2+} + N_2H_4 + 4OH^- \rightarrow 2Ni + N_2\uparrow + 4H_2O \quad (1)$$

$$2CO^{2+} + N_2H_4 + 4OH^- \rightarrow 2Co + N_2\uparrow + 4H_2O \quad (2)$$

$$Co + Ni \rightarrow CoNi \quad (3)$$

The microwave heating can improve the nucleation rate to form CoNi alloy nuclei around the sites, CoNi alloy nuclei formed on the shell of MWCNTs grows through the continuous surface to form CoNi alloy nanoparticles. With the increasing atomic ratios of CoNi/MWCNTs, CoNi alloy nuclei formed on the shell of MWCNTs increases, a large amount of CoNi alloy nanoparticle aggregates are formed, which leads to the quasi-spherical CoNi alloy nanoparticle over the entire external MWCNT surface, as shown in parts (b) and (c) of Fig. 5.

3.3. Magnetic measurement

Magnetic properties of the samples were investigated at room temperature using a VSM with an applied field $-10\,kOe \leq H \leq 10\,kOe$. Fig. 6 shows the hysteresis loops for samples with 3, 7, 12 and 18 at%. The values of the coercivity (Hc) and the saturation magnetization (Ms) of field for all samples were listed in Table 1. It can be seen that the Hc increases with increase of the particle size from 15 nm to 37 nm, and decreases with increase of the particle size from 37 nm to 48 nm. According to the theory of the magnetic domain [26], there is a critical size ds of single domain particles. When the particle size (D) is smaller than ds, the magnetic particles are single domain particles. When D is larger than ds, the magnetic particles are multi-domain particles. The Hc of single domain particles increases with the increase of D, while the Hc of the multi-domain particles decreases with the increase of D. The critical size ds of CoNi alloy nanopaticle is about 40 nm reported in literature [27]. So when the particle size of CoNi alloy nanoparticle increased from 15 nm to 48 nm, the single domain turned to multi-domain, the coercivity increased and reached to maximum at the size of 37 nm, and then decreased. The Ms of CoNi/MWCNT nanocomposites shown in Table 1 also increases with the increase of the particle size from 15 nm to 37 nm, this is mainly related to the increase of the content of CoNi alloy nanoparticle in the composites, and the surface disorder contribution is lower with the largest particles duo to their lower surface/volume ratio, then their magnetiazation is higher. While the Ms decreases when the particle size increases to 48 nm, which maybe results from domain wall displacement in the multi-domain structure, magnetic anisotropy of crystals, the surface-to-volume ratio and the surface defect of the nanocrystals [28,29].

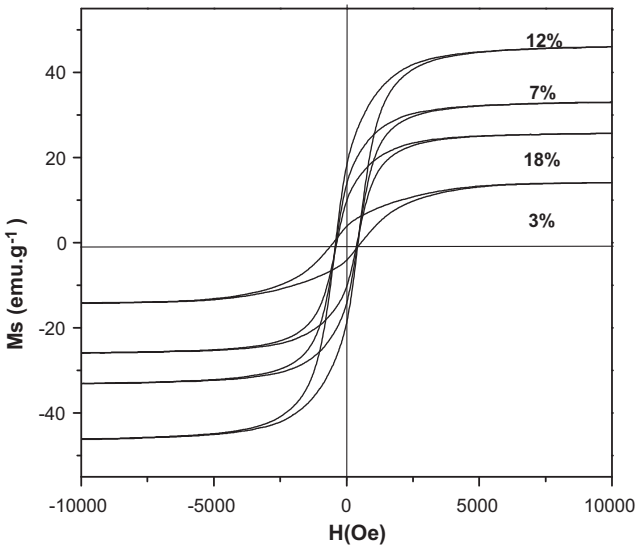

Fig. 6. The hysteresis loops of different atomic ratios of CoNi/MWCNTs

4. Conclusions

CoNi alloy nanoparticles with average diameters in the range of 15–48 nm attached on the carbon nanotubes were synthesized by microwave-assisted method. CoNi alloy nanoparticles were fcc structure, quasi-spherical and dispersed uniformly on the surface of MWCNTs. The size of the nanoparticles can be controlled through adjusting the atomic ratio of metal to carbon in the mixed acetate solution. Magnetic measurement shows that the coercivity and the saturation magnetization vary with the change of the particle size. Both the Hc and the Ms of the samples increased with the increase of the particle size from 15 nm to 37 nm, and decreased from 37 nm to 48 nm. These results demonstrate that the microwave-assisted method is promising for preparation of size-controlled magnetic alloy nanoparticles attached on MWCNTs for magnetic storage and the ultra high-density magnetic recording applications.

Acknowledgments

We thank Anhui Provincial Natural Science Foundation (No.070414179) and National Natural Science Foundation (No. 20901003) of the People's Republic of China for financial support.

References

[1] S. Pane, E. Gomez, J. Garcia-Amoros, D. Velasco, E. Valles, Appl. Surf. Sci. 253 (2006) 2964–2968.
[2] S.L. Pan, Z.G. An, J.J. Zhang, G.Z. Song, Mater. Chem. Phys. 124 (2010) 342–346.
[3] A. Foyet, A. Hauser, W. Schafer, J. Solid State Electrochem. 12 (2008) 47–55.
[4] Y. Rheem, B.Y. Yoo, W.P. Beyermann, N.V. Myung, Nanotechnology 18 (2007) 125204–125209.
[5] L.F. Sun, J.M. Mao, Z.W. Pan, B.H. Chang, W.Y. Zhou, G. Wang, L.X. Qian, S.S. Xie, Appl. Phys. Lett. 74 (1999) 644–646.
[6] M. Wen, Y.F. Wang, F. Zhang, Q.S. Wu, J. Phys. Chem. C 113 (2009) 5960–5966.
[7] P. Toneguzzo, G. Viau, O. Acher, F. Guillet, E. Bruneton, F. Fievet-Vincent, F. Fievet, J. Mater. Sci. 35 (2000) 3767–3784.
[8] N. Galvez, E. Valero, M. Ceolin, S. Trasobares, M. Lopez-Haro, J.J. Calvino, J.M. Domınguez-Vera, Inorg. Chem. 49 (2010) 1705–1711.
[9] P. Elumalai, H.N. Vasan, M. Verelst, P. Lecante, V. Carles, P. Tailhades, Mater. Res. Bull. 37 (2002) 353–363.
[10] L. Pei, K. Mori, M. Adachi, Langmuir 20 (2004) 7837–7843.
[11] E. Hao, R.C. Bailey, G.C. Schatz, J.T. Hupp, S. Li, Nano Lett. 4 (2004) 327–330.
[12] Y. Ramaye, S. Neveu, V. Cabuil, J. Magn. Magn. Mater. 289 (2005) 28–31.
[13] S. Thongmee, H.L. Pang, J.B. Yi, J. Ding, J.Y. Lin, L.H. Van, Acta Mater. 57 (2009) 2482–2487.
[14] D. Ung, G. Viau, C. Ricolleau, F. Warmont, P. Gredin, F. Fievet, Adv. Mater. 17 (2005) 338–344.
[15] M.J. Hu, Y. Lu, S. Zhang, S.R. Guo, B. Lin, M. Zhang, S.H. Yu, J. Am. Chem. Soc. 130 (2008) 11606–11607.
[16] L.P. Zhu, H.M. Xiao, S.Y. Fu, Eur. J. Inorg. Chem. (2007) 3947–3951.
[17] S. Pane, E. Gomez, J. Garcıa-Amoros, D. Velasco, E. Valles, J. Electroanal. Chem. 604 (2007) 41–47.
[18] X.J. Zhang, W. Jiang, D. Song, J.X. Liu, F.S. Li, Mater. Lett. 62 (2008) 2343–2346.
[19] Z.P. Dong, K. Ma, J.G. He, J.J. Wang, R. Li, J.T. Ma, Mater. Lett. 62 (2008) 4059–4061.
[20] Q.F. Liu, W.C. Ren, Z.G. Chen, B.L. Liu, B. Yu, F. Li, H.T. Cong, H.M. Cheng, Carbon 46 (2008) 1417–1423.
[21] H.Q. Cao, M.F. Zhu, Y.G. Li, J. Solid State Chem. 179 (2006) 1208–1213.
[22] D. Shi, J.P. Cheng, F. Liu, X.B. Zhang, J. Alloys Compd. 502 (2010) 365–370.
[23] H.Q. Wu, Q.Y. Wang, Y.Z. Yao, C. Qian, X.J. Zhang, X.W. Wei, J. Phys. Chem. C. 112 (2008) 16779–16783.
[24] H.Q. Wu, Q. Wang, Y.Z. Yao, C. Qian, P.P. Cao, X.J. Zhang, X.W. Wei, Mater. Chem. Phys. 113 (2009) 539–543.
[25] G. Viau, F. Fievet-Vincent, F. Fievet, Solid State Ionics 84 (1996) 259–270.
[26] G.D. Tang, D.L. Hou, M. Zhang, L.H. Liu, L.X. Yang, C.F. Pan, X.F. Nie, H.L. Luo, J. Magn. Magn. Mater. 251 (2002) 42–49.
[27] C. Luna, M.P. Morales, C.J. Serna, M. Vazquez, Nanotechnology 14 (2003) 268–272.
[28] M.A. Gonzalez-Fernandez, T.E. Torres, M. Andres-Verges, R. Costo, P. Presa, C.J. Serna, M.P. Morales, C. Marquina, M.R. Ibarra, G.F. Goya, J. Solid State Chem. 182 (2009) 2779–2784.
[29] H. Li, H.Z. Wu, G.X. Xiao, Powder Technol. 198 (2010) 157–166.